JOURNAL OF SOLID STATE CHEMISTRY 83, 150–157 (1989)

Mössbauer Study of Vacancy Distribution in $CaMn_{1-x}Fe_xO_{3-y}$ ($x = 0.5, 0.6$)

J. FONTCUBERTA AND M. A. CRUSELLAS

Departament Física Fonamental, Universitat de Barcelona, Diagonal 647, Barcelona 08028, Spain

J. RODRÍGUEZ-CARVAJAL

Institut Laue-Langevin, BP 156x, 38042 Grenoble-Cedex, France

AND M. VALLET, J. ALONSO, AND J. GONZÁLEZ-CALBET

Departamento Química Inorgánica, Facultad de Químicas, Universidad Complutense, Madrid 28040, Spain

Received January 17, 1989; in revised form June 13, 1989

$CaMn_{1-x}Fe_xO_{3-y}$ samples prepared in air contain several types of intergrowing microdomains as observed by electron microscopy. Using Mössbauer spectroscopy we have proved the existence of three differently coordinated Fe^{3+} cations and we propose a model for microdomain composition and distribution that accounts well for Mössbauer and electron microscopy data. Here, we study in detail the $x = 0.5$ and 0.6 terms of this series. We show that for this composition the brownmillerite-type domains are large enough to suppress superparamagnetism at room temperature. According to our own earlier suggestions, room-temperature magnetic ordering is observed for these samples.

Introduction

Compositional variations, either chemical substitutions or nonstoichiometry, in a compound can be accommodated in a very complex manner. In some cases, the foreign atoms or vacancies can be randomly distributed or ordered in some particular way. In other cases, phase segregation can happen. Indeed, in some perovskite systems ABO_{3-y} it has been shown that the anionic vacancies are ordered in such a way that three-dimensional microdomains exist in the sample. X-ray diffraction is unable to reveal the existence of such ordering but electron diffraction and microscopy have undoubtably shown the existence of microdomains and have been used to determine the vacancy arrangement in each domain (*1, 2*).

Vallet-Regí *et al.* (*3*) reported an electron microscopy study of the $CaMn_{1-x}Fe_xO_{3-y}$ system. These authors showed that for $x = 0.2$ there exist perovskite-type domains (PTD) with a doubled axis arranged in three different orientations through the crystal.

0022-4596/89 $3.00

For $x = 0.4$, a more complicated microdomain structure is observed. Electron microscopy reveals the coexistence of PTD and brownmillerite-type domains (BTD), both with the long axis oriented at random in the directions ⟨100⟩ of the cubic perovskite substructure. Note that in the PTD ($CaMnO_3$-type) the transition-metal cation is octahedrally coordinated but in the BTD ($Ca_2Fe_2O_5$-type) there are octahedrally and tetrahedrally coordinated metallic cations in a ratio 1 : 1.

As mentioned above, X-ray powder diffraction fails to reveal the nature of this complex microstructure. Only a broadening of Bragg reflections is detected. Consequently, a local probe should be helpful to fully characterize these samples. Recently, we used (*4*) Mössbauer spectroscopy to study the $x = 0.2, 0.3, 0.4$ terms of the $CaMn_{1-x}Fe_xO_{3-y}$ system when quenched from 1400°C, and from this analysis a model of vacancy ordering emerged. In the brownmillerite $Ca_2Fe_2O_5$, the structure is built up by octahedra and tetrahedra sharing an apical corner, and this pair of polyhedra can be viewed as the structural brick. It was suggested (*4*) that the octahedral–tetrahedral (OT) units of the BTD grow as isolated entities, increasing their concentration as the total amount of oxygen vacancies in the sample increases, which in turn rises with the concentration of Fe cations (x). The composition of the BTD deduced from the analysis of Mössbauer spectra was $Ca_2Fe_2O_5$, thus showing that Mn cations do not participate in the brownmillerite-type domains.

In pure $Ca_2Fe_2O_5$, the atomic magnetic moments are ordered at room temperature, and a hyperfine magnetic splitting is observed in Mössbauer spectra (*5*). The lack of apparent magnetic order at room temperature, in our $CaMn_{1-x}Fe_xO_{3-y}$ sample ($x = 0.4$), was interpreted on the basis of a superparamagnetic behavior of isolated OT units. Indeed, low-temperature Mössbauer spectra reveal the existence of the typical magnetic fields of $Ca_2Fe_2O_5$ (*4*). Consequently, it was suggested that for $x > 0.4$ it should be possible to observe the hyperfine magnetic splittings even at room temperature.

Recently, we performed (*6*) the structural study of the $0.5 < x < 0.9$ terms of this series by using X-ray diffraction and electron microscopy. Here, we report the Mössbauer study of the $x = 0.5$ and $x = 0.6$ terms of the $CaMn_{1-x}Fe_xO_{3-y}$ system. We show that, in agreement with the results so far obtained for the $x < 0.4$ terms, these materials are also constituted by intergrowth of PTD and BTD. Our present data confirm the previously reported suggestions and we perform a general analysis of the microdomain structure of all the investigated terms of the system ($0.2 < x < 0.6$). It must be noticed that for the sample $x = 0.6$, electron diffraction and microscopy (*6*) reveal the presence of some crystals with microdomains of the *G*-phase (GTD), of ideal composition $A_3B_3O_8$ (*7*). As we demonstrate below, the presence of this phase does not invalidate our analysis.

Experimental

$CaMn_{1-x}Fe_xO_{3-y}$ samples ($x = 0.5, 0.6$) were prepared from stoichiometric mixtures of $CaCO_3$, $MnCO_3$, and α-Fe_2O_3. The mixture was heated at 1100°C in air for 48 hr to decompose the carbonates and, then, fired at 1400°C for 16 hr. The black materials thus obtained were homogeneous under the optical microscope.

Powder X-ray diffraction patterns were carried out on a Siemens D-500 diffractometer using Cu$K\alpha$ radiation and silicon as internal standard. Both samples, $x = 0.5$ and 0.6, gave patterns that could be assigned to an average cubic perovskite-like structure, although a slight broadening of Bragg reflections was observed. Unit cell parameters are summarized in Table I.

TABLE I

CHEMICAL ANALYSIS DATA AND UNIT CELL PARAMETERS

x (nom.)	Chemical composition	a (Å)
0.5	$CaFe^{3+}_{0.5}Mn^{3+}_{0.13}Mn^{4+}_{0.37}O_{2.685}$	3.775
0.6	$CaFe^{3+}_{0.6}Mn^{3+}_{0.15}Mn^{4+}_{0.25}O_{2.625}$	3.784

Total amounts of calcium, iron, and manganese were confirmed by atomic absorption spectrometry. The oxidation state of iron in the samples was determined by chemical analysis by using a $K_2Cr_2O_7$ 0.1 *N* solution after dilution in 3 *N* HCl with an excess of Mohr salt. It is observed that all iron is in a trivalent state of oxidation. The amounts of both Mn^{4+} and Mn^{3+} were determined, as proposed by Fyfe (*8, 9*), by dissolving the sample in hydrochloric acid and adding potassium iodine solution in the presence of acetylacetone. The iodine liberated was determined by titration with $Na_2S_2O_3$ solution in the presence of starch. Chemical compositions thus obtained are listed in Table I.

Mössbauer spectra have been recorded using a conventional constant acceleration drive system. The spectra were recorded at two different velocity ranges: ±12 and ±4 mm/sec in order to get a better resolution of the central part of the spectra. The data of Table II refer to parameters obtained from the fit of the spectra recorded in the +12 mm/sec velocity range. For the $x = 0.6$ sample, we also include the relevant parameters obtained from the low-velocity range spectrum. In this fit, the hyperfine parameters of the magnetic phase have been constrained to be equal to those obtained for the high-velocity range. Data of Table II show the internal consistency of both sets of results.

Results and Discussion

Figures 1a and 1b show the room-temperature Mössbauer spectra of the $x = 0.5$ and $x = 0.6$ samples. Both spectra reveal the existence of a paramagnetic phase together with a magnetically ordered phase whose relative intensity increases from $x = 0.5$ to $x = 0.6$. The magnetic phase of $x = 0.6$ has been fitted by using a set of two hyperfine sextets which are broadened by a Lorentzian distribution of hyperfine magnetic fields. The convolution of Lorentzian distribution (HWHM = ΔH, where HWHM is the half-width-at-half-maximum) of Lorentzian intensity lines (HWHM = Γ) produces a new Lorentzian function whose width is related to the widths of both Lorentzian distributions. We have assumed Γ to be the natural line width and we have fitted ΔH.

In Table II are included the relevant parameters obtained from the fit of the magnetic phase. ISM1, QSM1, HF1 and ISM2, QSM2, HF2 are the isomer shift, quadrupole shift, and hyperfine magnetic field for

TABLE II

RELEVANT MÖSSBAUER PARAMETERS

x	ISM1	ISM2	IS1	IS2	IS3	QSM1	QSM2	QS1	QS2	QS3	HF1	HF2
0.5	0.20 (19)	0.40 (19)	0.32 (24)	0.20 (17)	0.29 (21)	0.51	−0.74	0.61	1.49	1.07	349(19)	367(56)
0.6	0.18 (33)	0.40 (33)	0.34 (13)	0.21 (18)	0.30 (6)	0.72	−0.71	0.64	1.51	1.07	351(19)	387(67)
0.6[a]	Fixed	Fixed	0.33 (16)	0.20 (14)	0.29 (7)	Fixed	Fixed	0.65	1.51	1.09	Fixed	Fixed

Note. IS and QS are in millimeters per second. The hyperfine magnetic fields and the HWHM of their distributions (ΔH) are given in KOe units. IS are referred to α-Fe. The relative area in percentage of each subspectrum is given within parentheses. The estimated error of the area parameters are about 5%.

[a] These parameters are obtained from the lower velocity range spectrum.

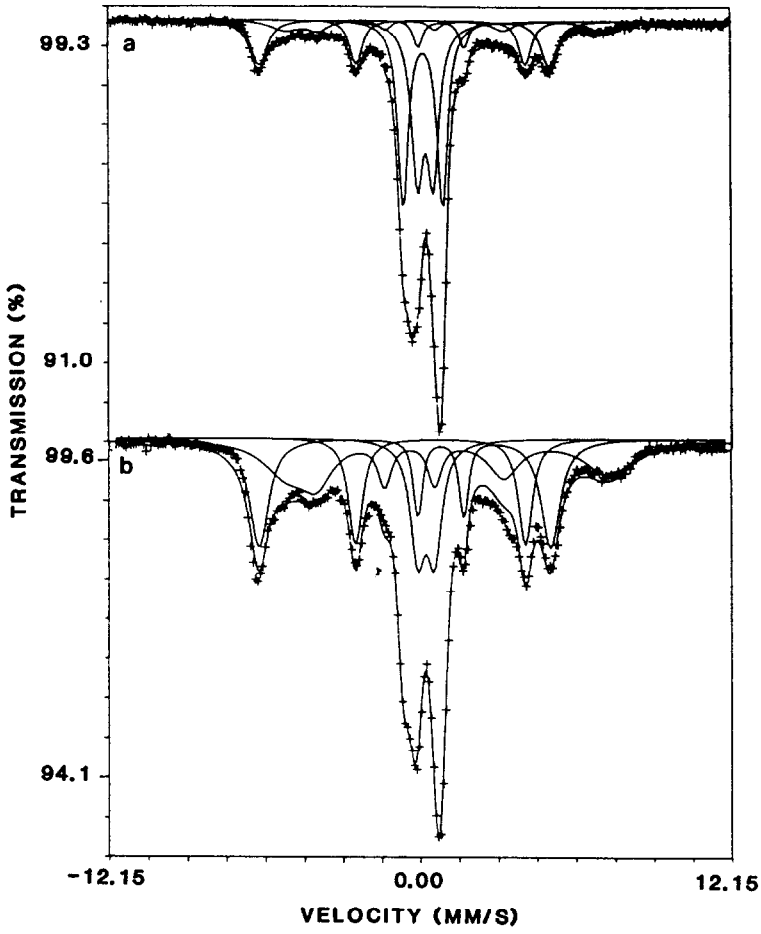

FIG. 1. Room-temperature Mössbauer spectra of $CaFe_xMn_{1-x}O_{3-y}$ samples for $x = 0.5$ (a) and $x = 0.6$ (b).

sextets 1 and 2, respectively. Within the experimental error both sextets have the same relative intensity (see Table II). The IS values are typical of tetrahedrally coordinated Fe^{3+} (ISM1 $\approx$ 0.18 mm/sec) and octahedrally coordinated Fe^{3+} (ISM2 $\approx$ 0.40 mm/sec) (*10*). Consistent with this finding are the hyperfine magnetic field values, being smaller for the tetrahedral coordination as usually found. Note that the quadrupole splitting for both sites have opposite signs. For the $x = 0.5$ sample, a similar analysis holds, but the lower relative intensity of the magnetically ordered phase (= 38%) gives a larger error of the fitted parameters.

At this point it is worth emphasizing that the measured Mössbauer parameters are in excellent agreement with those reported for $Ca_2Fe_2O_5$. Not only the hyperfine magnetic fields but also the quadrupole splitting values are very similar (*5*).

The central part of the spectrum for $x = 0.6$ has been fitted by using three quadrupole split lines. The corresponding parameters are included also in Table II. Note that IS1 = 0.34 mm/sec and IS2 = 0.20 mm/sec

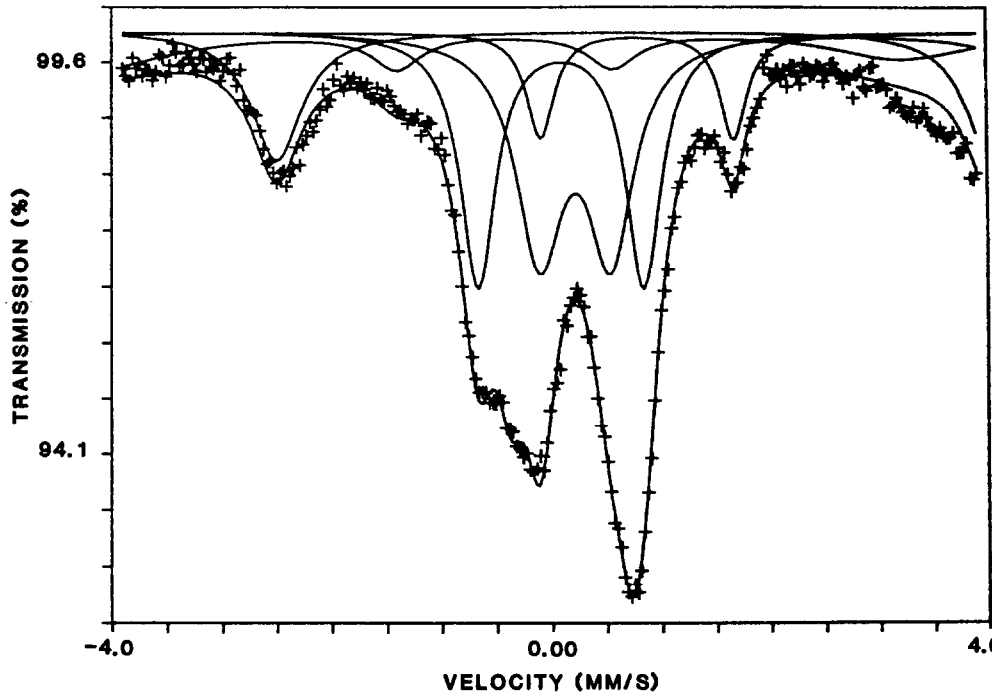

FIG. 2. Room-temperature Mössbauer spectrum of $x = 0.6$ sample measured at a narrower velocity range.

values are typical of Fe^{3+} in octahedral and tetrahedral coordination, respectively. The value of IS3 = 0.30 mm/sec which lies between those of IS1 and IS2 can be attributed to Fe^{3+} in fivefold oxygen coordination. A similar analysis has been previously done (*4*) for $x = 0.2$, 0.3, and 0.4 samples of the same substitutional series.

To check the accuracy of the fit, we have remeasured the central part of the spectrum in the ±4 mm/sec velocity range (see Fig. 2). To perform this fit, we have used as fixed parameters those corresponding to the magnetic subspectra already obtained from the fit of the spectra of Fig. 1. The results are also included in Table II. Note that they compare very well with those obtained from the first spectrum.

The quadrupole splitting values (QS1, QS2, QS3) measured for the nonmagnetic part of the spectra are close to those previously reported for the $x = <0.4$ term of this system. In fact, as shown in Fig. 3, the quadrupole splitting of the octahedrally coordinated Fe^{3+} ions increases when the concentration of Mn^{4+} ions in the PTD increases. This result should have been expected on the basis of the consideration of the asymmetric surrounding caused by the existence of Mn^{4+} cations.

The discussion of these results starts from the consideration of the area data in Table II. The relative area of the subspectra associated with tetrahedrally coordinated Fe^{3+} ions (Fe_{tet}), increases when going from $x = 0.5$ to $x = 0.6$; $I(Fe_{tet}) = 36\%$ and 51%,

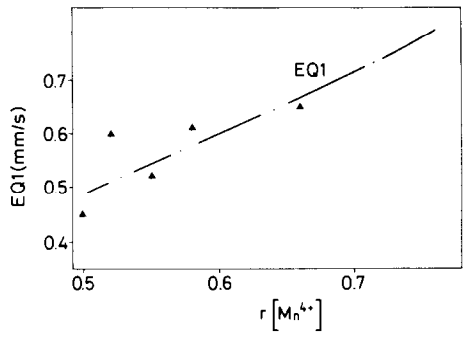

FIG. 3. Dependence of the quadrupole splitting of the octahedrally coordinated Fe^{3+} ions on the concentration of Mn^{4+} ions in the PTD. Data for $x < 0.5$ are taken from Ref. (*4*).

respectively. This result is in agreement with the results obtained by electron microscopy, where brownmillerite-type domains (BTD), which contain OT units, are more abundant when x value increases (*4*, *6*). We previously suggested (*4*) that the OT units can be spatially arranged to form BTD and we have proposed a structural formula that reflects this particular arrangement:

$$CaMn^{3+}_{1-x-z}Mn^{4+}_{z}Fe^{oct}_{x-t-v}Fe^{v}_{v}Fe^{tet}_{t}O_{3-y} = q[CaMn^{3+}_{0.5-m}Fe^{oct}_{m}Fe^{tet}_{0.5}O_{2.5}]_{OT} + (1-q)[CaMn^{3+}_{1-p-r}Mn^{4+}_{r}Fe^{oct}_{p-w}Fe^{v}_{v}O_{3-\delta}]_{PTD}. \quad (1)$$

From the chemical analysis the overall oxygen vacancy concentration (y) and the total concentration of Fe(x) and Mn(z) are known. By assuming similar recoilless factors for all iron atoms, the relative amounts of Fe^{3+} in fivefold, octahedral, and tetrahedral coordinations can be deduced from the Mössbauer spectra. Of course, it is far from obvious that octahedral, tetrahedral, or penta-coordinated Fe^{3+} ions all have the same recoilless fractions. However, in the brownmillerite $CaFe_2O_5$ it is observed that the ratio of the areas of the Fe^{oct} and Fe^{tet} lines have the right value, thus suggesting that their f values are indeed very similar. However, we are extending this result to the Fe^{v} ions. The consistency of all our data appears to support this hypothesis. With these data, the charge neutrality condition, and the equivalence of both members of Eq. (1), it is possible to deduce (*4*) the concentration of OT units (q), the relative amount of Mn^{4+} ions (r) and of fivefold coordinated Fe^{3+} ions (w), and the oxygen vacancy concentration (δ) in PTD.

For the sample $x = 0.6$, in which GTD exist, the interpretation of q is not directly related to the amount of BTD, but it is clear that q represents the concentration of OT units despite the particular spatial arrangement of them. The *G*-phase (*7*) presents a structure intermediate between the perovskite and brownmillerite: along the b axis exists a staking sequence of octahedral and tetrahedral layers of type: OOTOOTOOTOOT. . . , then the OT units are arranged in planes alternating with an octahedral layer. The Mössbauer signal arising from GTD contributes to both parts of the second member of Eq. (1); this fact prevents obtaining the concentration of GTD.

In order to perform the compositional analysis of the samples it should be considered that the OT units can reveal a magnetically split spectrum when they are arranged in a BTD of sufficient size. The magnetic part of the spectrum must be added to the paramagnetic one to take into account the correct concentration of OT units. In Table III we show the q, r, w, and d values deduced in such a way. Figure 4 shows the dependence of some of these parameters on the substitutional parameter (x). We have included, for completeness, some of the data reported in our previous paper (*4*).

From Fig. 4 it is clear that the OT concentration in the samples increases continuously when the total amount of Fe increases. For lower concentrations of OT units (q) their magnetic interaction is weak and they show a superparamagnetic behavior; consequently, the Mössbauer spectra

TABLE III

PARAMETERS OBTAINED FROM THE SOLUTION OF THE EQUATIONS (1)

x	q	r	w	δ
0.5	0.36	0.58	0.17	0.21
0.6	0.62	0.66	0.095	0.17

Note. q is the relative concentration of OT units in the sample; r is the Mn^{4+} concentration in the PTD; w is the Fe^{3+} concentration in the PTD; δ is the oxygen vacancy concentration in the PTD.

at room temperature does not show any magnetic splitting. As we previously reported, at low temperature a magnetic split spectrum is shown by the $x < 0.5$ samples. As q becomes larger, free rotation of the magnetic moments of the OT units is avoided and the hyperfine magnetic field is apparent (bulk $Ca_2Fe_2O_5$ is magnetically ordered at room temperature). As mentioned at the beginning of this discussion, the coexistence of two magnetic hyperfine fields arises from the Fe^{tet} and Fe^{oct} ions of the OT units in the BTD.

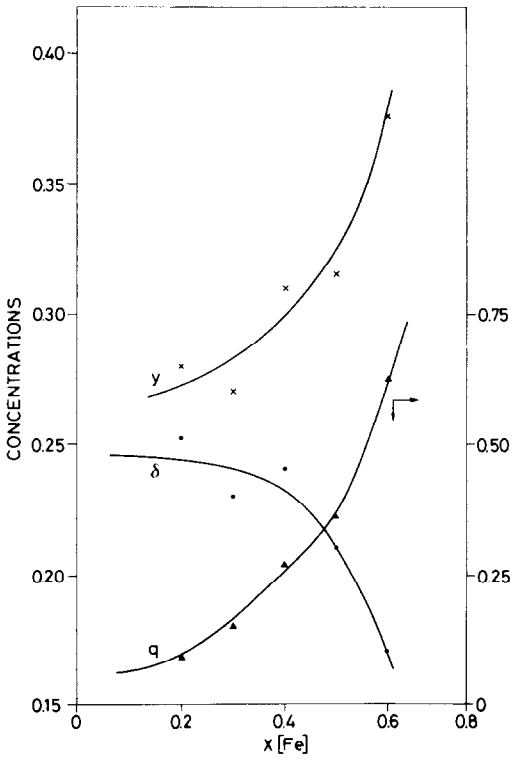

FIG. 4. Dependence of the compositional parameters on the substitution rate. y, δ, and q are the concentrations of oxygen vacancies in the sample and in the PTD and BTD, respectively. Data for $x < 0.5$ are taken from Ref. (*4*).

Note also that the total amount of oxygen vacancies increases when substituting Mn by Fe, but they are not randomly distributed over the sample. The $\delta(x)$ dependence displayed in Fig. 4 reveals that the oxygen vacancies have a tendency to order in OT units as their concentration becomes larger, thus leading to more stoichiometric PTD.

Finally, according to our data, the compositional formulas of the samples $x = 0.5$ and $x = 0.6$ are:

$$x = 0.5: \quad 0.36[CaFeO_{2.5}] + 0.64[CaMn^{3+}_{0.20}Mn^{4+}_{0.58}Fe^{v}_{0.17}O_{2.79}]$$

$$x = 0.6: \quad 0.62[CaFeO_{2.5}] + 0.38[CaMn^{3+}_{0.40}Mn^{4+}_{0.66}Fe^{v}_{0.095}O_{2.83}].$$

Therefore, the reported results confirm the predictions already made by us (*4*, *6*) in the following sense:

(1) As the concentration of Fe increases the total amount of oxygen vacancies increases.

(2) As the concentration of oxygen vacancies is increased, they tend to be ordered in OT units.

(3) The OT units are structural elements for building BTD. Therefore, as expected, when the concentration of OT units is large enough, bulk magnetic properties of $Ca_2Fe_2O_5$ (antiferromagnetic ordering at room temperature) are apparent and the magnetic splitting in Mössbauer spectra are clearly seen.

References

1. M. A. ALARIO FRANCO, J. M. GONZÁLEZ-CALBET, M. VALLET-REGÍ, AND J. C. GRENIER, *J. Solid State Chem.* **49**, 219 (1983).

2. J. M. González-Calbet, M. Vallet-Regí, and M. A. Alario Franco, *J. Solid State Chem.* **60,** 320 (1985).

3. M. Vallet-Regí, J. M. González-Calbet, J. Verde, and M. A. Alario Franco, *J. Solid State Chem.* **57,** 197 (1985).

4. J. Rodríguez, J. Fontcuberta, G. Longworth, M. Vallet-Regí, and J. M. González-Calbet, *J. Solid State Chem.* **73,** 57 (1988).

5. S. Geller, R. W. Grant, and U. Gonser, *Prog. Solid State Chem.* **5,** 5 (1971).

6. J. M. González-Calbet, M. Vallet-Regí, J. Alonso, J. Rodríguez, and J. Fontcuberta, *J. Solid State Chem.*, in press (1989).

7. J. C. Grenier, J. Darriet, M. Pouchard, and P. Hagenmuller, *Mater. Res. Bull.* **11,** 1219 (1976).

8. W. S. Fyfe, *Nature (London)* **121,** 190 (1949).

9. W. S. Fyfe, *Anal. Chem.* **23,** 174 (1951).

10. F. Menil, *J. Phys. Chem. Solids* **46,** 763 (1985).